Spatial and temporal trends in extreme rainfall in a savannah-forest transition zone: the case of the Marahoué catchment area

Comment [DK1]: Title should be not so long.

ABSTRACT

Keywords: Climatic extremes; Extremesprecipitations;Floods;Modified Mann–Kendall;Droughts;Rainfall trend analysis; Marahoué catchment

Numerous studies have addressed future changes in hydroclimatic extremes using a variety of approaches. However, trends in extreme precipitation intensities remain less well known, especially for design precipitation intensities used in stormwater infrastructure design. Hence the importance of identifying flood and low-water extremes in the Marahoué catchment in Côte d'Ivoire. Given their importance, trends in the series of extremes were studied using the modified Mann Kendall test. Trends were studied for various short-term rainfall durations at eight stations. Spatial distribution using the IDW interpolation method enabled climate indices to be distributed over the Marahoué basin. Spatial analysis of precipitation indices over four decades shows a trend towards an intensification of extreme events (Rx1day and Rx5day), accompanied by a decrease in prolonged drought periods (CDD, R10 and R20). Temporal analysis of extreme rainfall indices reveals a variety of trends depending on the station and type of index. However, most of the trends obtained are insignificant. The use of decades makes it easy to update intensity-duration-frequency curves, and is more practical and understandable for engineers. The results of this study underline the importance of monitoring climate change through localized analyses and approaches, and of adapting water resource management strategies to better cope with the growing risks associated with extreme rainfall.

1. INTRODUCTION

Climates in different parts of the world are characterized by their variability, which has an impact on socio-economic activities. This variability has increased since the 1950s, and particularly during the latest decade, mainly because of the increased concentration of anthropogenic greenhouse gases in the atmosphere as argued by some authors (Hegerl *et al*., 2007, Stott *et al*., 2010, Trenberth *et al.*, 2007, Min *et al*., 2011). These climatic variations have had repercussions on climate extremes worldwide, according to the Sixth Assessment Report of the Intergovernmental Panel on Climate Change (IPCC, 2021). Several studies have recently been carried out on changes in global and regional precipitation extremes (Baidya *et al.*, 2008; IPCC *et al.*, 2013; Soltani *et al.*, 2016). Recent studies in Africa, when analyzing daily climate in terms of trends and extreme indices revealed some significant increases and decreases in annual precipitation, increases in longest wet spells, increases in high daily precipitation amounts and average rainfall intensity (Alexander *et al.*, 2006, Collins, 2011).

Climate extremes, such as heavy rainfall, have a significant impact on human societies and ecosystems particularly in ecological transition zones such as those between savannah and forest. In these zones, climatic variations can lead to marked changes in hydrological regimes, with consequences for water resource management and agriculture. Indeed, these savannah-forest transition zones are sensitive to

climatic variations, such as rainfall. Changes in rainfall can cause the boundary between savannah and forest to shift. According to many authors (Knapp *et al.*, 2008; Heisler-White *et al.*, 2009; Kulmatiski and Beard, 2013; Zhang *et al.*, 2019) the global increase in extreme precipitation observed in recent decades is set to affect the structure and functioning of terrestrial ecosystems.

The Marahoué catchment, located in a transition zone between climate (equatorial-tropical) and vegetation (savannah-forest), is particularly sensitive to climatic variations and human disturbance. In indeed, Irie et al (2016) in the basin showed alternating wet (1970-1980) and dry (1981-2000) periods. The dry period resulted in a rainfall deficit of 15% to 37%. Moreover, they observed a return to the wet since 2000 in the basin. Over the last few decades, the Marahoué catchment area has had to cope with flooding and run-off in urban areas. The most catastrophic flood to date was in September 2018, which displaced several people and affected around 3,500 in Bouaflé and 3,500 to 6,112 in Zuénoula. The main cause of this flooding is linked to an exceptional rainfall situation that occurred between 18 August and 12 September 2018 in the Marahoué basin. Rainfall in 2018 was 92% higher than in 2017 and 136% higher than the average for 2001-2017.

In such a climatic context, the aim of this study in the Marahoué catchment is to analyses the variability of rainfall extremes using static indices in order to help build resilience and plan adaptation to flooding.

2. MATERIAL AND METHODS

2.1. STUDY AREA

The study area is the Marahoué river catchment. It is located in central-western Côte d'Ivoire between longitudes 5.5°W and 7.5°W, and latitudes 6.5°N and 9.5°N. It is a sub-basin of the Bandama river. The study basin is a sub-basin of the Bandama river.The north of the Marahoué basin covers the administrative regions of Kabadougou and Bagoué. The central part includes the Worodougou and Béré regions. In the south of the basin, the regions of Haut-Sassandra and Marahoué.The climatic context of the basin is dominated by two climate zones: the Sudanese climate zone (tropical regime) and the Baouleen climate zone (transitional equatorial regime). (Irié, 2017).

Figure 1: Geographical location of the Marahoué catchment (BENIAMBIE, 2025)

Datasets

Table 1. Rainfall stations selected for the study.

Vegetation	Climatic zone	Stations	Code	Latitude	Longitude
Savannah area	**Sudanese climate**	Boundiali	1090006400	9.516	- 6.483
		Séguélon	1090017600	9.356	-7.122
		Dianra	1090340000	8.761	-6.242
		Kani	1090011700	8.489	-6.603
		Mankono	1090014800	8.059	- 6.189
Forest areas	**Baoulean climate**	Séguéla	1090017500	7.960	- 6.674
		Zuénoula	1090022200	7.429	- 6.043
		Bouaflé	1090005200	6.982	-5.753

The data used are daily rainfall amounts. They were recorded over the period 1980 to 2020 and were made available by the Direction of National Meteorology (SODEXAM). The characteristics of the rain gauging stations that recorded the data used in this study are shown in Table 1.

Methods

In this section, the methods used will enable the extreme rainfall indices to be extracted and their spatial and temporal variation to be analysed.

- **Extraction of extreme rainfall indices**

The RClimDex software follows two main stages in the extraction of extreme weather indices: data quality control and index calculation.

Data quality control: This aims to correct errors in the daily data. The number of daily observations is limited to 365-366 days per year, and February to 28 days. These adjustments guarantee the reliability of the data.

Calculation of indices: Among the 27 indices defined by the ETCCDI, 5 rainfall indices representative of rainfall extremes are retained, such as consecutive dry days (CDD), days with precipitation ≥10 mm (R10) or ≥20 mm (R20), maximum precipitation in one day (Rx1Day), and over 5 days (Rx5Day) (table 2). This method enables in-depth analysis of extreme weather events.

Table 2: Rainfall indices characterizing rainfall extremes

Index Class	Identification	Names	Definitions	Units
Duration indices	**CDD**	Consecutive dry days	Maximum number of consecutive days with daily precipitation < 1 mm	Day
Frequency indices	**R10**	Number of days with precipitation ≥ 10 mm		Day
	R20	Number of days with precipitation ≥ 20 mm		Day
Intensity indices	**Rx1Day**	Maximum daily rainfall	Monthly maximum 1-day precipitation	mm
	Rx5Day	Maximum 5-day rainfall	Maximum total precipitation over 5 consecutive rainy days of the year	mm

- **Inverse Distance Weighting (IDW)**

The inverse distance interpolation method (IDW) was used to highlight the spatial variability of extreme rainfall indices. IDW is a local, exact, and deterministic method (Hadi and Tombul, 2018). The interpolation

method estimates a value locally as a function of the distances between the estimation point and the neighbouring measured points (Rebai *et al*., 2007). Each known point contributes to the estimate with a weight that is inversely proportional to the distance. The Zj value to be estimated is given by the following relationship:

$$Z_j = \left(\sum_{i=1}^{m} \frac{Z_i}{(d_{ij}+S)^P}\right) / \left(\sum_{i=1}^{m} \frac{1}{(d_{ij}+S)^P}\right)$$

Zj: Value to be estimated at point j of variable Z. Zi: Known value, measured at point i of variable Z, dij: Distance between points i and j, S: Smoothing factor, P: Weight assigned to distance dij

- **Mann-Kendall's Classic Test**

Comment [DK2]: If using only modified test then discuss about modified only that will be enough.

This test checks if there is a trend in the time series data. It is a non-parametric test robust to the influence of extremes and allows its application to biased variables (Hamed, 2008). More particularly, this nonparametric trend test is the result of an improvement of the test first studied by Mann (1945) then taken up by Kendall (1970) and finally perfected by Helsel and Hirsch (2002). Mann-Kendall's test is based on the sign of the difference between the ranks of a time series. Given a time, series of X = (x_1,x_2…..x_n), Mann-Kendall's statistics is given as:

$$S = \sum_{i=1}^{n-1} \sum_{j=i+1}^{n} a_{ij} \qquad (2)$$

where:

$$a_{ij} = sign(x_j - x_i) = sign(R_j - R_i) \qquad (3)$$

$$a_{ij} = \begin{cases} 1 \; if \; x > 0 \\ 0 \; if \; x = 0 \\ -1 \; if \; x < 0 \end{cases} \qquad (4)$$

and R_j, R_I are respectively, the ranks of the observations of the series. Under the hypothesis that the data are independent and identically distributed. Kendall (1970), gives the mean and variance of the above S-test statistics:

$$E(S) = 0 \qquad (5)$$

$$Var(S) = \frac{n(n-1)(2n+5)}{18} \qquad (6)$$

where **n**is the size of the series. The existence of equal observations in the series leads to a reduction in the variance of **S**, which becomes:

$$Var(s) = \frac{n(n-1)(2n+5)}{18} - \frac{\sum_{j=1}^{m} t_j(t_j-1)(2t_j+5)}{18} \qquad (7)$$

where **m** is the number of groups of equal observations and **t j**, number of equal observations in group **j**.

We can normalize statistics of the test to get a new **Z** test statistic:

$$Z = \begin{cases} \frac{(S-1)}{\sqrt{V_0(S)}} & si \; S > 0 \\ 0 & si \; S = 0 \\ \frac{(S+1)}{\sqrt{V_0(S)}} & si \; S > 0 \end{cases} \qquad (8)$$

A positive (or negative) value of Z indicates an ascending (or descending) trend and its significance is compared to the critical value α or significance threshold of the test.

- **Modified Mann-Kendall Test**

The presence of autocorrelation in the data can seriously affect the power of statistical tests by overestimating the statistical significance of trends. This autocorrelation is usually generated by a cyclic recurrence in the evolution of the data reflecting a dependence on external phenomena (variation in recharging, application cycles). A complementary approach to the classic Mann-Kendall test is thus proposed in order to take into account this phenomenon of autocorrelation. The principle is based on a modification of Mann-Kendal's S test rather than modifying the data itself:

$$Var_{\rho}(S) = \gamma * Var_{\rho=0}(S) \qquad (9)$$

where $\gamma$is a corrective factor applied to the variance.

Two methods are noted in the literature to estimate this corrective factor.

•[**25**] suggest correcting the Mann-Kendall test as follows:

$$\gamma = 1 + 2 * \frac{\rho_1^{n+1} - n\rho_1^2 + (n-1)\rho_1}{n(\rho_1 - 1)^2} \qquad (10)$$

where $\rho_1$denotes the autocorrelation of order 1

•[**26**] propose an empirical formula specifically calculated to correct Mann-Kendall's statistics:

$$\gamma = 1 + \frac{2}{n(n-1)(n-2)} \sum_{k=1}^{n-1} (n-k)(n-k-1)(n-k-2)\rho_k \qquad (11)$$

In this study, the corrective factor from Hamed (1998) was used because the tests carried out by Renard (2006) on the power of these methods, show that the modification proposed by Hamed and Rao is slightly better under the AR (1) hypothesis than the formula of Yue and Wang. Indeed, it takes into account the autocorrelation of the regression residuals calculated at the different ranks if they are significant.

3. RESULTS AND DISCUSSION

- **Analysis of spatial variation in extreme rainfall index**

CDD (Consecutive dry days)

Figure 2 shows the spatial evolution by decade of the maximum number of consecutive dry days (CDD) over the period 1983-2022. There is considerable decadal variability in the CDD index in the Marahoué basin. The 1983-1992 decade was the most critical, with values ranging from 86 to 96 days, particularly in the north-western part of the basin. The following decades showed a relative stabilization, followed by a slight resumption of dry periods in recent years. Overall, the CDD index follows a north/south gradient.

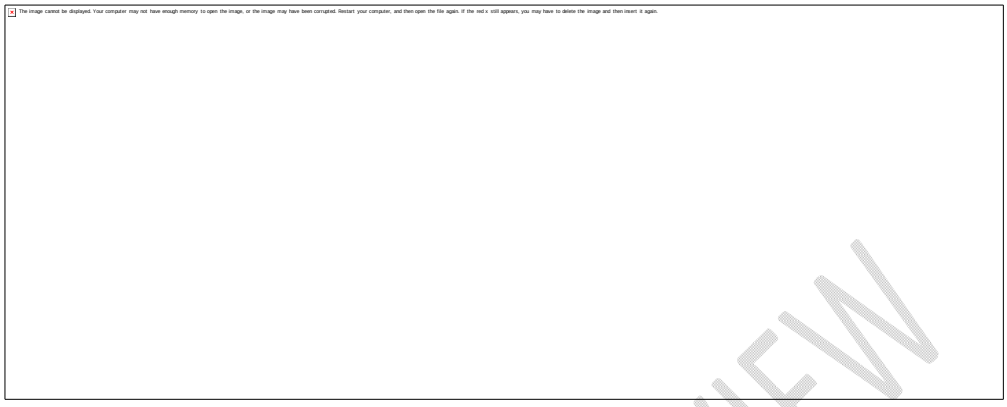

Figure 2: Decadal evolution of the CDD index in the Marahoué catchment (1983-2022) (BENIAMBIE, 2025)

R10 (Number of days with precipitation ≥ 10 mm)

Spatial trends in the number of days with precipitation in excess of 10 mm are shown in Figure 3. Over the decade 1983-1992, there was a high concentration of intense rainfall days in the north-west. Between 1993 and 2002, the distribution of heavy rainfall shifted towards the northeast. During the 2003–2012 decade, figure 3 shows a general decrease in R10 index. The map for the last decade shows a slight upturn in intense rainfall in the northern areas of the Marahoué catchment.

Figure 3: Decadal evolution of the R10 index in the Marahoué catchment (1983-2022) (BENIAMBIE, 2025)

R20 (Number of days with precipitation ≥ 20 mm)

The evolution of the R20 index in the Marahoué basin shows a downward trend between 1983 and 2012, followed by a recent recovery (Figure 4). The recurrence of the number of days with rainfall above 20 mm is notable over the periods 1983-1992 and 2013-2022. The center of the catchment is most affected by the drop in rainfall days over 20 mm between 1993-2012. Areas in the south show R20 indices close to those observed in the north.

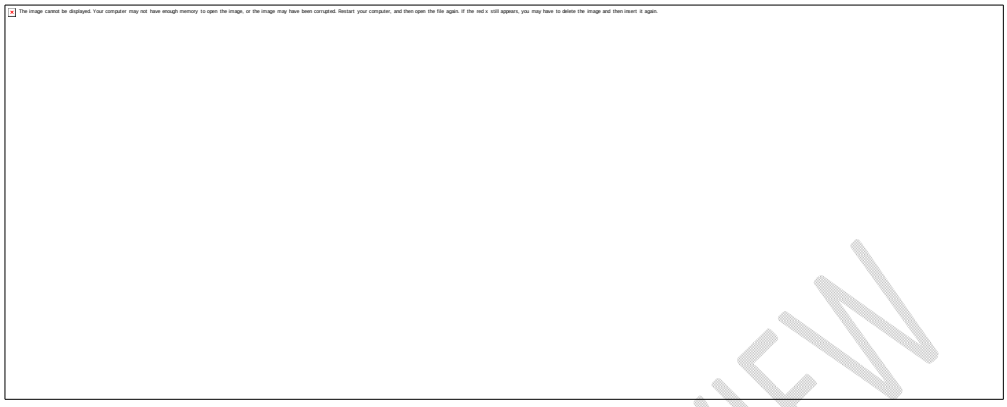

Figure 4: Decadal evolution of the R20 index in the Marahoué catchment (1983-2022) (BENIAMBIE, 2025)

Rx1day (Maximum daily rainfall)

The Figure 5 shows the spatial distribution of the Rx1day index. During the first decade, the lowest rainfall amounts were observed in the north of the basin, precisely in the localities covered by the Kani station (63 to 70 mm). The highest maximum daily rainfall amounts were recorded at the Mankono station in the center of the catchment (91 to 98 mm). For the last two decades, the Kani station has retained the lowest values (70 mm - 77mm). As for maximum indices, they are found at Dianra (98 mm - 105mm from 2003 to 2012) and at the Séguélon, Séguéla and Mankono stations (91 mm - 98 mm from 2013 to 2022).

Figure 5: Decadal evolution of the Rx1day index in the Marahoué catchment (1983-2022) (BENIAMBIE, 2025)

Rx5day (Maximum 5-day rainfall)

Spatial analysis reveals a significant increase in the intensity of extreme precipitation over 5 days (Figure 6). The low Rx5day index values of 1983-1992 have given way to high, homogeneous indices throughout the basin. The central area of the Marahoué catchment was the first to be affected by this increase in 1993-2002. Since 2003-2022, the phenomenon has become more widespread throughout the basin, reflecting a strengthening of the extreme rainfall regime.

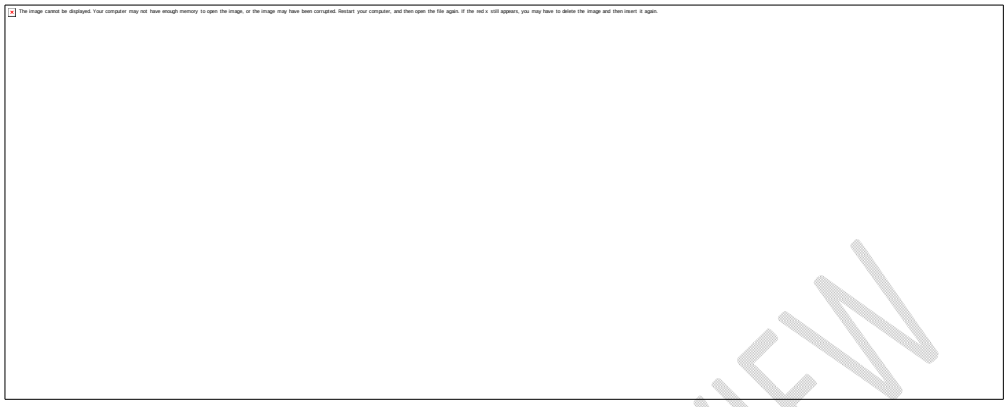

Figure 6: Decadal evolution of the Rx5day index in the Marahoué catchment (1983-2022) (BENIAMBIE, 2025)

- **Analysis of temporal variation in extreme rainfall index**

CDD (Consecutive dry days)

Table 6 shows the results of the Mann-Kendall test applied to the CDD index series for the Marahoué catchment. The majority of stations show non-significant trends. Only two stations (Bouaflé and Dianra) show significant trends. Significant trends are downward.

Table 3: Trends in the CDD index at the rainfall stations used over the period 1983-2022

Index	Stations	Zc	p-value	Sen slope	Trend	Sign. at α
CDD	**Bouaflé**	-3,384	0,001	-1,040	**- -**	**TS**
	Boundiali	-1,330	0,183	-0,400	**- -**	TNS
	Dianra	-2,251	0,024	-0,781	**- -**	**TS**
	Kani	0,026	0,979	0,000	**+ +**	TNS
	Mankono	0,643	0,520	0,167	**+ +**	TNS
	Séguéla	0,286	0,775	0,085	**+ +**	TNS
	Séguélon	-0,380	0,704	-0,118	**- -**	TNS
	Zuénoula	-0,616	0,538	-0,200	**- -**	TNS

TS: Significant trend; TNS: Not significant trend; ++: Upward trend; --: Downward trend; α=5%.

R10 (Number of days with precipitation ≥ 10 mm) and R20 (Number of days with precipitation ≥ 20 mm)

Results of the Mann-Kendall test applied to the R10 and R20 index series for the Marahoué catchment. The R10 indices showed increases at some stations, but only a significant trend was observed (Bouaflé). The evolution of the R20 index remained stable over the period 1983-2022, with no notable trends at all stations.

Table 4: Trends in the R10 and R20 index at the rainfall stations used over the period 1983-2022

Stations	Index	Zc	p-value	Sen slope	Trend	Sign. at α

Bouaflé	**R10**	2,245	0,025	0,240	**+ +**	**TS**
Boundiali		0,486	0,627	0,034	**+ +**	TNS
Dianra		0,146	0,884	0,000	**+ +**	TNS
Kani		-1,686	0,092	-0,179	**- -**	TNS
Mankono		1,235	0,217	0,104	**+ +**	TNS
Séguéla		1,215	0,224	0,118	**+ +**	TNS
Séguélon		-0,852	0,394	-0,105	**- -**	TNS
Zuénoula		0,088	0,930	0,000	**+ +**	TNS
Bouaflé	**R20**	-0,050	0,960	0,000	**- -**	TNS
Boundiali		-0,197	0,844	0,000	**- -**	TNS
Dianra		0,789	0,430	0,043	**+ +**	TNS
Kani		-0,450	0,652	-0,015	**- -**	TNS
Mankono		-1,051	0,293	-0,091	**- -**	TNS
Séguéla		1,688	0,091	0,106	**+ +**	TNS
Séguélon		-1,864	0,062	-0,154	**- -**	TNS
Zuénoula		-0,356	0,722	0,000	**- -**	TNS

TS: Significant trend; TNS: Not significant trend; ++: Upward trend; --: Downward trend; α=5%.

Rx1day (Maximum daily rainfall) and Rx5day (Maximum 5-day rainfall)

The table shows trends in the Rx1day and Rx5day rainfall indices for various stations. The Rx1day index shows a strong upward trend at most stations in the basin, but only the Dianra, Kani, Séguéla and Séguélon stations are significant at the 5% threshold. As for the Rx5day index, the significant trends recorded are at the Dianra, Kani and Séguélon stations for the increasing trend, and Bouaflé for the decreasing trend.

Table 5: Trends in the Rx1day and Rx5day index at the rainfall stations used over the period 1983-2022

Stations	Index	Zc	p-value	Sen slope	Trend	Sign. at α
Bouaflé	**Rx1day**	-2,716	0,007	-0,867	**- -**	**TS**
Boundiali		-0,827	0,409	-0,274	**- -**	TNS
Dianra		2,222	0,026	0,804	**+ +**	**TS**
Kani		2,924	0,003	0,702	**+ +**	**TS**
Mankono		0,196	0,844	0,085	**+ +**	TNS
Séguéla		2,754	0,006	0,956	**+ +**	**TS**
Séguélon		2,367	0,018	1,218	**+ +**	**TS**
Zuénoula		0,629	0,530	0,232	**+ +**	TNS
Bouaflé	**Rx5day**	-2,112	0,035	-1,100	**- -**	**TS**
Boundiali		-0,362	0,717	-0,212	**- -**	TNS
Dianra		2,868	0,004	1,119	**+ +**	**TS**
Kani		2,346	0,019	1,005	**+ +**	**TS**
Mankono		0,432	0,666	0,325	**+ +**	TNS
Séguéla		1,730	0,084	0,850	**+ +**	TNS
Séguélon		2,976	0,003	1,387	**+ +**	**TS**
Zuénoula		-0,269	0,788	-0,153	**- -**	TNS

TS: Significant trend; TNS: Not significant trend; ++: Upward trend; --: Downward trend; α=5%.

4. Discussion

The results of extreme rainfall indices in the Marahoué catchment revealed significant spatio-temporal dynamics, partly aligned with trends observed in other West African regions. The results showed a relatively downward trend in consecutive dry days at the Bouaflé, Dianra, Boundiali, Séguélon and Zuénoula stations. These results reflect a reduction in prolonged dry periods in these zones, favored by an

upturn in rainfall. According to Royer-Gaspard *et al.* (2019), this phenomenon could be attributed to a redistribution of rainfall patterns, favored by global climatic factors such as intensified evaporation and increased atmospheric humidity, known to alter hydrological cycles. According to Konaté *et al.* (2023), a climatic split has been identified, with a transition to dry periods as early as 1982 in the north and 1983 in the south of Côte d'Ivoire, characterized by a decrease in total rainfall and an increase in dry periods. Moreover, the 1983-1992 decade, identified as critical with prolonged dry spells in the north-western part of the catchment, corresponds to a phase of widespread drought in West Africa. This phenomenon may be linked to global climatic anomalies, in particular to an intensification of El Niño episodes during this period. According to Nicholson (2001) and Janicot *et al.* (2008), El Niño years are often associated with a reduction in rainfall in Sahelian and sub-Sahelian regions, contributing to an increase in drought periods in the Marahoué basin.

The evolution of the R10 and R20 indices highlights a generalized decrease in days of heavy rainfall between 1983 and 2012, followed by a recent recovery. These results concur with those of Sanogo *et al.* (2015), who observed a decrease in rainfall in West Africa, associated with an increased concentration of intense rainfall in short periods. This trend mirrors the observations of Konaté et al. (2023), who noted an increase in extreme rainfall events over the past 15 years in Côte d'Ivoire, with an increased concentration in coastal and urban areas. The spatial distribution shows a northeastward migration of heavy rainfall between 1993 and 2002, which could be explained by changes in local atmospheric regimes, as described by Sylla *et al.* (2016) in their studies of monsoon dynamics in West Africa. This recent recovery may be linked to phenomena such as the Niño, which favor wetter monsoon conditions in West Africa. Janicot *et al.* (2008) have shown that the Niño intensifies atmospheric convection, thereby increasing the frequency and intensity of rainfall.

The intensification of extreme precipitation events (Rx1day and Rx5day) observed in the Marahoué basin reflects global trends in the intensification of extreme events documented by IPCC (2021). This intensification could be linked to an increase in the atmosphere's capacity to retain moisture as global temperatures rise (Clausius-Clapeyron effect). The results show that stations such as Dianra, Séguéla and Kani show significant upward trends, suggesting an increased sensitivity of these localities to extreme climatic events. These observations concur with the findings of Koné et al (2020), who documented an increase in flooding in Côte d'Ivoire linked to exceptional rainfall. The intensification of rainfall over 5 consecutive days, particularly since 2003, is also in line with the work of Panthou *et al.* (2014), who showed that rainfall extremes in West Africa have been on the increase since the 1990s, despite a general decrease in annual rainfall totals.

These results underline the need to integrate recent climate data and future projections into water resource planning. The trends observed, particularly the increase in extreme precipitation, call for proactive management to limit the impact on water infrastructures and local communities.

5. Conclusion

Comment [DK3]: Font is changed in this section.

Analysis of extreme rainfall indices in the Marahoué catchment over the period 1983-2022 reveals significant spatial and temporal variations, testifying to the growing impacts of climate change. The results show a gradual reduction in dry days (CDD index) at some stations, while indices linked to intense precipitation (R10, R20, Rx1day and Rx5day) show significant increases, particularly in recent decades.

These observations confirm an intensification of extreme events, consistent with regional trends in West Africa, as reported by other studies. The evolution of indices highlights a redistribution of rainfall patterns, with a marked north-south gradient and significant differences between stations.

These changes present major challenges for water resource management, agriculture and the resilience of hydraulic infrastructures. They also underline the urgency of integrating adaptation measures, notably by strengthening early warning systems and

raising awareness among local communities. Finally, these results provide an important basis for further analysis, by integrating climate models and extending the study to other catchments for a more global vision.

6. Références

[1]. Alexander, L. V., Zhang, X., Peterson, T. C., Caesar, J., Gleason, B., Klein Tank, A. M. G., ... & Vazquez-Aguirre, J. L. (2006). *Global observed changes in daily climate extremes of temperature and precipitation*. Journal of Geophysical Research: Atmospheres, 111(D5).

[2]. Baidya, S. K., Shrestha, M. L., & Sheikh, M. M. (2008). *Trends in daily climatic extremes of temperature and precipitation in Nepal*. Journal of Hydrology and Meteorology, 5(1), 38-51.

[3]. Collins, M. (2011). *Temperature variability over Africa*. Journal of Climate, 24(14), 3649-3666.

[4]. Hadi, S. and Tombul, M. (2018) Long-Term Spatiotemporal Trend Analysis of Precipitation and Temperature over Turkey: Spatiotemporal Precipitation and Temperature Trend over Turkey. *Meteorological Applications*, 25, 445-455.

[5]. Hamed KH, Rao R. A modified Mann-Kendall trend test for autocorrelated data. J. Hydrol. 1998; 204, 182-196.

[6]. Hamed KH. Trend detection in hydrologic data: The Mann-Kendall trend test under the scaling hypothesis, Journal of Hydrology. 2008; 349: 350-363.

[7]. Hegerl, G. C., Zwiers, F. W., Braconnot, P., Gillett, N. P., Luo, Y., Marengo Orsini, J. A., ... & Stott, P. A. (2007). Understanding and Attributing Climate Change. In *Climate Change 2007: The Physical Science Basis*. Contribution of Working Group I to the Fourth Assessment Report of the Intergovernmental Panel on Climate Change (pp. 663-745). Cambridge University Press.

[8]. Heisler-White, J. L., Blair, J. M., Kelly, E. F., Harmoney, K., & Knapp, A. K. (2009). "Contingent productivity responses to more extreme rainfall regimes across a grassland biome." *Global Change Biology*, 15(12), 2894–2904.

[9]. Helsel DR, Hirsch RM. Statistical Methods in Water Resources Techniques of Water Resources Investigations, Livre 4, chapitre A3. Enquête géologique des États-Unis. 522 pages. 2002.

[10]. Intergovernmental Panel on Climate Change (IPCC). (2013). *Climate Change 2013: The Physical Science Basis*. Contribution of Working Group I to the Fifth Assessment Report of the Intergovernmental Panel on Climate Change. Cambridge University Press.

[11]. Intergovernmental Panel on Climate Change. *Climate Change 2021: The Physical Science Basis*. Contribution of Working Group I to the Sixth Assessment Report of the Intergovernmental Panel on Climate Change. Edited by V. Masson-Delmotte, P. Zhai, A. Pirani, S.L. Connors, C. Péan, S. Berger, N. Caud, Y. Chen, L. Goldfarb, M.I. Gomis, M. Huang, K. Leitzell, E. Lonnoy, J.B.R. Matthews, T.K. Maycock, T. Waterfield, O. Yelekçi, R. Yu, and B. Zhou. Cambridge University Press

[12]. IPCC (2021). "Climate Change 2021: The Physical Science Basis. Contribution of Working Group I to the Sixth Assessment Report of the Intergovernmental Panel on Climate Change." Cambridge University Press.

[13]. Irié. G. R. (2017). Impacts des changements climatiques sur les ressources en eau du bassin versant de la Marahoué (Côte d'Ivoire). Thèse de Doctorat de l'Université Nangui Abrogoua, Côte d'Ivoire, 190 p.

[14]. Janicot, S., Trzaska, S., & Poccard, I. (2001). "Summer Sahel-ENSO teleconnection and decadal time scale SST variations." *Climate Dynamics*, 18, 303-320.

[15]. Kendall MG. Rank correlation methods, 202 pp., Griffin, London.

[16]. Knapp, A. K., Beier, C., Briske, D. D., Classen, A. T., Luo, Y., Reichstein, M., Smith, M. D., Smith, S. D., Bell, J. E., Fay, P. A., Heisler, J. L., Leavitt, S. W., Sherry, R., Smith, B., & Weng, E. (2008). "Consequences of more extreme precipitation regimes for terrestrial ecosystems." *BioScience*, 58(9), 811–821

[17]. Konate, D.; Didi, S.R.; Dje, K.B.; Diedhiou, A.; Kouassi, K.L.; Kamagate, B.; Paturel, J.-E.; Coulibaly, H.S.J.-P.; Kouadio, C.A.K.; Coulibaly, T.J.H. Observed Changes in Rainfall and Characteristics of Extreme Events in Côte d'Ivoire (West Africa). *Hydrology* 2023, *10*, 104. https://doi.org/10.3390/hydrology10050104

[18]. Koné, B., & al. (2020). "Analyse des inondations en milieu urbain en Côte d'Ivoire : Cas de la ville d'Abidjan." *Revue Ivoirienne des Sciences et Technologie*, 36, 50-65.

[19]. Kulmatiski, A., & Beard, K. H. (2013). "Woody plant encroachment facilitated by increased precipitation intensity." *Nature Climate Change*, 3, 833–837.

[20]. Mann H. B. Nonparametric tests against trend, Econometrica. 1945; 13, 245-259.

[21]. Min, S. K., Zhang, X., Zwiers, F. W., &Hegerl, G. C. (2011). Human contribution to more-intense precipitation extremes. *Nature*, 470(7334), 378-381.

[22]. Nicholson, S. E. (2001). "Climatic and environmental change in Africa during the last two centuries." *Climate Research*, 17(2), 123-144.

[23]. Panthou, G., Vischel, T., & Lebel, T. (2014). "Recent trends in the regime of extreme rainfall in the Central Sahel." *International Journal of Climatology*, 34(15), 3998-4006.

[24]. Rebai, N., Slama, T. and Turki, MM (2007) Evaluation of different spatial interpolation methods for producing a DTM from topographic data in a GIS. XYZ, 110, 19-28.

[25]. Renard B. - Détection et prise en compte d'éventuels impacts du changement climatique sur les extrêmes hydrologiques en France. Thèse de l'Institut National Polytechnique de Grenoble. Unité de Recherche Hydrologie-Hydraulique, Cemagref (Lyon). 2006

[26]. Royer-Gaspard, P., Andréassian, V., Thirel, G., & Perrin, C. (2019). "Comment l'évolution de l'évaporation potentielle impacte les sécheresses." *Colloque UNESCO-SHF : Sécheresses 2019, Paris 11-12 et 13 décembre 2019*.

[27]. Sanogo, S., Fink, A. H., Omotosho, J. A., Ba, A., Redl, R., & Ermert, V. (2015). "Spatio-temporal characteristics of the recent rainfall recovery in West Africa." *International Journal of Climatology*, 35(15), 4589-4605.

[28]. Soltani, S., Modarres, R., & Sarhadi, A. (2016). *Assessment of climate variations in temperature and precipitation extreme events over Iran*. Theoretical and Applied Climatology, 125, 101-114.

[29]. Stott, P. A., Gillett, N. P., Hegerl, G. C., Karoly, D. J., Stone, D. A., Zhang, X., & Zwiers, F. (2010). Detection and attribution of climate change: a regional perspective. *Wiley Interdisciplinary Reviews: Climate Change*, 1(2), 192-211.

[30]. Sylla, M. B., Giorgi, F., Coppola, E., & Mariotti, L. (2016). "Uncertainties in daily rainfall over Africa: Assessment of gridded observation products and evaluation of a regional climate model simulation." *International Journal of Climatology*, 36(1), 476-491.

[31]. Trenberth, K. E., Fasullo, J., & Smith, L. (2007). Trends and variability in column-integrated atmospheric water vapor. *Climate Dynamics*, 24(7-8), 741-758.

[32]. Zhang, L., Wylie, B. K., Ji, L., Gilmanov, T. G., & Tieszen, L. L. (2019). "Climate-driven interannual variability in net ecosystem exchange in the northern Great Plains grasslands." *Rangeland Ecology & Management*, 62(5), 478–490.